JACS
JOURNAL OF THE AMERICAN CHEMICAL SOCIETY

ARTICLE

pubs.acs.org/JACS

Chain Packing in Glassy Polymers by Natural-Abundance $^{13}C-^{13}C$ Spin Diffusion Using 2D Centerband-Only Detection of Exchange

Manmilan Singh and Jacob Schaefer*

Department of Chemistry, Washington University, St. Louis, Missouri 63130, United States

Supporting Information

ABSTRACT: The proximities of specific subgroups of nearest-neighbor chains in glassy polymers are revealed by distance-dependent $^{13}C-^{13}C$ dipolar couplings and spin diffusion. The meassurement of such proximities is practical even with natural-abundance levels of ^{13}C using a 2D version of centerband-only detection of exchange (CODEX). Two-dimensional CODEX is a relaxation-compensated experiment that avoids the problems associated with variations in $T_1(C)$'s due to dynamic site heterogeneity in the glass. Isotropic chemical shifts are encoded in the t_1 preparation times before and after mixing, and variations in T_2's are compensated by an S_0 reference (no mixing). Data acquisition involves acquisition of an S_0 reference signal on alternate scans, and the active control of power amplifiers, to achieve stability and accuracy over long accumulation times. The model system to calibrate spin diffusion is the polymer itself. For a mixing time of 200 ms, only $^{13}C-^{13}C$ pairs separated by one or two bonds (2.5 Å) show cross peaks, which therefore identify reference intrachain proximities. For a mixing time of 1200 ms, 5 Å interchain proximities appear. The resulting cross peaks are used in a simple and direct way to compare nonrandom chain packing for two commercial polycarbonates with decidedly different mechanical properties.

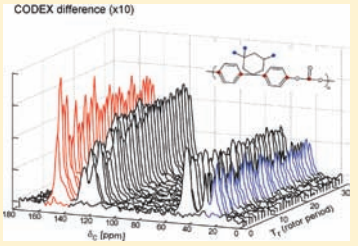

INTRODUCTION

We have recently examined chain packing in glassy polymers using specific stable-isotope labels and rotational-echo double resonance (REDOR).[1] Both distances and orientations have been observed[2] that are qualitatively consistent with the predictions of coarse-grained molecular dynamics models of the polymeric solid.[3] While the glass is disordered or randomly packed on a 50 Å distance scale, there is local order between specific subgroups on a 5 Å distance scale.[2,3] In this Article, we show that spin diffusion between ^{13}C's at natural abundance can also be used to detect interchain proximities and hence local order in bulk glassy polymers. The ^{13}C spin-exchange or spin-diffusion measurements are used to interpret chain packing for bisphenol A polycarbonate and trimethylcyclohexyl polycarbonate, two commercial glassy polymers with differing mechanical properties.

RESULTS AND DISCUSSION

2D CODEX. In standard CODEX, ^{13}C π pulses during the first preparation time, t_s, create chemical-shift-tensor coherences whose x- and y-components are stored prior to the mixing time.[4−7] If the shift-tensor orientation has remained unchanged during the mixing time, the ^{13}C π pulses during the second t_s period result in a signal that is stored, recovered, and detected as a Hahn echo. The same Hahn echo is observed regardless of whether t_m preceeds or follows t_z ($S = S_0$). However, if molecular or spin dynamics occurs during t_m but not during the much shorter t_z, refocusing is incomplete and ΔS is nonzero.

In the CODEX experiment of Figure S1, there are no pulses during t_s, and the effects of changes in shift-tensor orientations are removed by magic-angle spinning.[5,6] However, changes in isotropic chemical shifts during t_m contribute to ΔS, and in solids such changes are almost always due to spin diffusion (flip-flop spin exchange within $^{13}C-^{13}C$ pairs), not molecular exchange. However, in the event of slow molecular motion,[5] if the time scale of the slow motion is different from the 200 ms mixing time (say, a few milliseconds), then short t_m's will separate molecular and spin dynamics. If the two time scales are identical, perhaps the signature that the motion would interchange specific carbon sites but not others with a comparable distance separation, would help sort out molecular and spin dynamics without resorting to lowering the temperature.

The relationship between the 1D CODEX S and S_0 spectra is[7] $S/S_0 = Re\langle\exp(i(\varphi_1 + \varphi_2) - i(\varphi_1 + \varphi_1))\rangle = \langle\cos(\varphi_2 - \varphi_1)\rangle$, where φ_1 and φ_2 are the phase accumulations during t_s for a ^{13}C spin in isotropic chemical-shift environments 1 and 2, respectively, and the triangular bracket indicates an ensemble powder average. Environments 1 and 2 will be assumed connected by spin exchange only. Thus, the scaled CODEX difference spectrum ($1 - \Delta S/S_0 = S/S_0$) has a simple cosine modulation of the difference frequencies of ^{13}C's connected by spin diffusion.

In a 1D version of the CODEX experiment for spin diffusion,[5,6] all times are multiples of t_r (the rotor period), $t_m = N \cdot t_r$ and is hundreds of milliseconds, $t_z = m \cdot t_r$ and is a few milliseconds, and $t_s = n \cdot t_r$ with $n = 1$ or 2, for example. The timing of the d and f pulses is triggered externally by detection of the position of the rotor. The parameters N and m are integers

Received: October 10, 2010
Published: February 09, 2011

dx.doi.org/10.1021/ja109104f | J. Am. Chem. Soc. 2011, 133, 2626–2631

with $N \gg m$. If n is not fixed but incremented, the resulting 2D CODEX differences establish the chemical shifts of the spins engaged in exchange. When spinning sidebands are small, sampling in $t_1 = t_s$ can be asynchronous with respect to the rotor to increase the spectral width in the difference-frequency dimension.

Carbon-13 spin diffusion is sometimes enhanced by low-level proton irradiation during the mixing time.[8−10] Tightly coupled protons then provide a spin-dynamics medium so that frequency mismatches in $^{13}C-^{13}C$ exchanges are compensated by $^{1}H-^{1}H$ exchange. However, for relatively slow magic-angle spinning (less than 8 kHz), this step can be omitted for diffusion over distances of the order of 5 Å in 1 s.[11,12] In this situation, the $^{13}C-^{13}C$ frequency mismatches are compensated solely by changes in rotor-orientation-dependent static $^{1}H-^{13}C$ dipolar couplings. All of the 2D CODEX spectra reported here were obtained with a low-field spectrometer (100 MHz for protons) and 4 kHz magic-angle spinning. Spinning sidebands had negligible intensity, and the low spinning speed resulted in no substantive effect on ^{13}C spin diffusion.[13,14]

Another scheme to enhance ^{13}C spin diffusion uses multiple alternating depolarization of protons in dipolar contact with natural-abundance ^{13}C's.[15] Every ^{13}C spin depolarizes nearby proton spins multiple times in cross-polarization periods that alternate with the ^{13}C chemical-shift t_1 evolution periods.[16] Proton spin diffusion occurs during t_m and is monitored by a subsequent standard cross-polarization transfer to ^{13}C's with detection during t_2. Again, $^{13}C-^{13}C$ frequency mismatches are compensated by $^{1}H-^{1}H$ exchange. This scheme has important advantages over 2D CODEX in sensitivity, but a disadvantage for distance measurements due to a dependence of the $^{13}C-^{13}C$ spin-diffusion on the details of the $^{1}H-^{1}H$ network (vide infra).

A doubling of the number of acquisitions is necessary in 2D CODEX to obtain both S and S_0 under a constant total mixing time, $t_m + t_z$. However, this is time well spent because $T_1(C)$ corrections using single multiplicative factors are not possible for macromolecular solids with dynamic site heterogeneity.[17]

Sodium Propionate. The 2D CODEX spectra for sodium propionate for two values of the mixing time are shown in Figure 1. The pulse sequence of Figure S1 was used with $t_1 = t_s = nt_r/2$, $n = 0-63$. There are two t_1 periods, one before the long mixing time (t_m) and one after. This means that for a specific value of $nt_r/2$, the acquired signal is modulated by, for example, $\cos \Omega_1 t_s \cos \Omega_2 t_s$ in one scan, and $\sin \Omega_1 t_s \sin \Omega_2 t_s$ in the next.[18] The omega subscripts denote isotropic shifts before and after exchange during the mixing period. The sin and cos functions are selected by the choice of phase of the two 90° store pulses (Table S1).[6,18] The sum of the two scans therefore results in acquisition modulation by the difference frequency, $\Omega_2 - \Omega_1$. The modulation is always positive ($0 \le S \le S_0$) because the powder average of S cannot exceed that of S_0 in the absence of a coherence transfer. Thus, the sign of the frequency difference is not determined, and only the equivalent of a 2D power spectrum is obtained from the Fourier transform of either $\cos(\Omega_2 - \Omega_1)t_s$ or $\sin(\Omega_2 - \Omega_1)t_s$. When the difference frequency is zero ($S = S_0$), no exchange occurs, and no positive zero-frequency cross peaks appear in the 2D spectrum.

Cross peaks in 2D CODEX are connected by squares of shift versus shift difference. There are no peaks along the diagonal. Because of two t_1 samplings and the t_z filter, 2D CODEX is a pure-exchange experiment,[19] S and S_0 are measured identically with respect to $\pi/2$ pulse imperfections, and cross peaks close to the horizontal axis in contour plots can be detected without distortion.

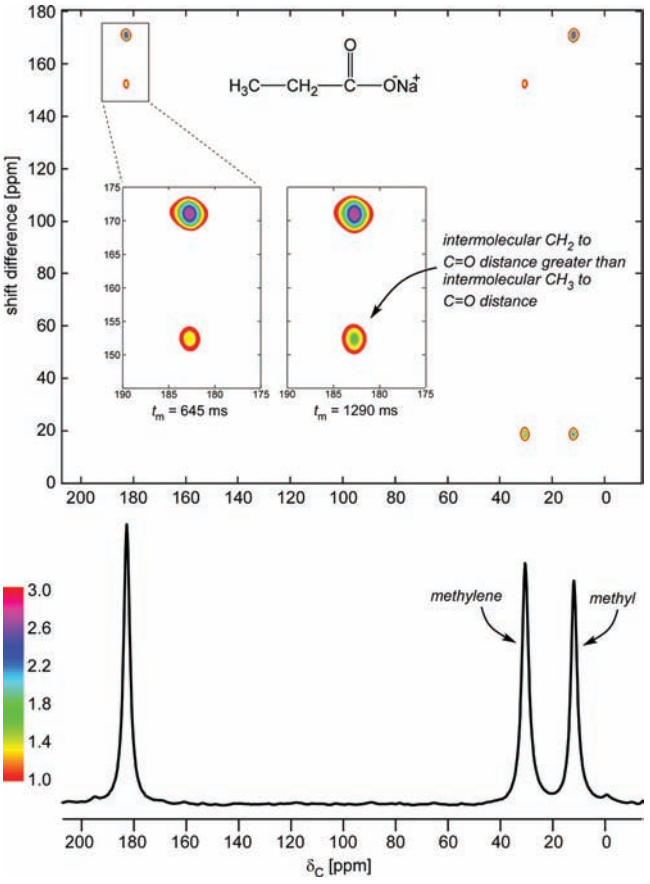

Figure 1. 2D CODEX difference spectrum of polycrystalline sodium propionate using the pulse sequence of Figure S1. The insets show expansions of the 182 ppm cross peaks for two values of the mixing time, t_m. The methyl−carboxyl cross peak has greater volume than the methylene−carboxyl cross peak for the 645 ms mixing time. This result is consistent with the intermolecular near-neighbor carboxyl−carbon distances to methyl and methylene carbons, as measured in the crystal structure (see the Supporting Information).

The intramolecular connectivities of all three carbons of sodium propionate are evident in Figure 1. For an intermediate mixing time $t_m = 645$ ms, the methyl−carboxyl (C3−C1) cross peak is greater than the methylene−carboxyl (C2−C1) cross peak, consistent with seven interatomic distances less than (or equal to) 5.433 Å for C3−C1 pairs, as compared to only three for C2−C1 pairs (Table S2). These distances were obtained from the X-ray crystal structure (see the Supporting Information). When the mixing time was increased to 1290 ms, the C2−C1 cross peak increases in volume more than the C3−C1 cross peak (insets), as the four C2−C1 pairs with distances between 5.509 and 6.019 Å (Table S2) contribute significantly to exchange.

Accurate calculations of 2D cross-peak volumes for different types of carbons require taking CH static dipolar couplings into account. Our purpose in showing sodium propionate spectra is not to generate a useful model to apply subsequently to polymer packing, but rather to illustrate the general features of 2D CODEX spectra. We have therefore not attempted a detailed accounting of spin diffusion within the complicated sodium propionate matrix.

The 2D CODEX signal acquisition suffers losses from the four imperfect store-and-read $\pi/2$ pulses, as well as from $T_1(C)$ decay during the mixing time. The S_0 spectrum shown in Figure 1

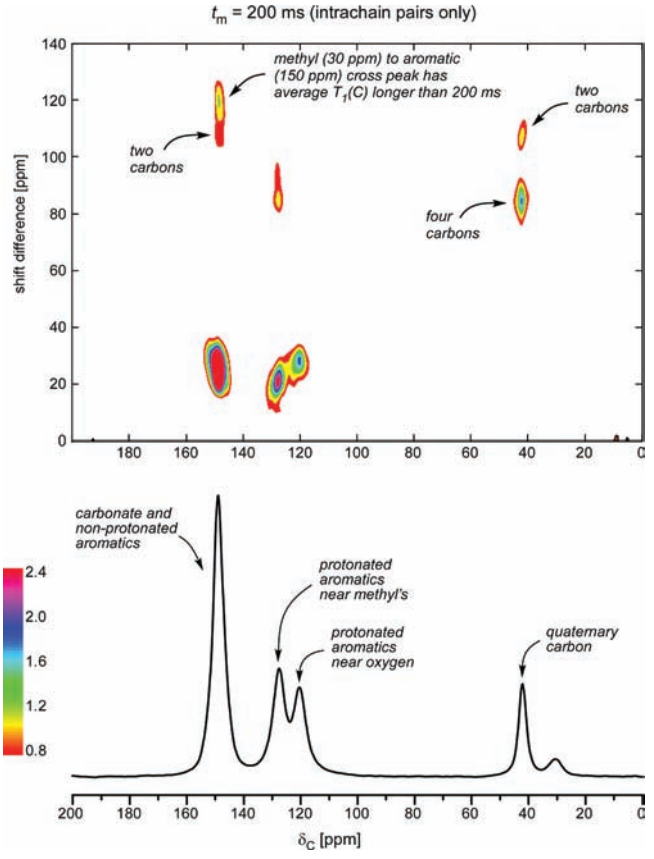

Figure 2. 2D CODEX difference spectrum of bisphenol A polycarbonate using the pulse sequence of Figure S1 with a mixing time of 200 ms. The methyl−carbon peak intensity at 30 ppm is reduced by a short methyl−carbon T_1; 30 ppm methyl−carbon cross peaks are below the selected threshold. The observed cross peaks arise from intrachain one and two-bond proximities for the short mixing time. The 42 ppm C_q cross-peaks arise from the four protonated-aromatic carbon and two nonprotonated aromatic carbon nearest neighbors (see structure in Figure 3, top).

(bottom) is reduced in sensitivity by a factor of 2.3 relative to that of a standard CPMAS experiment. The combination of alternate-scan S and S_0, with the active control of power amplifiers and transmission-line probe technology,[2] makes the long periods of data acquistion necessary for 2D CODEX practical.

Bisphenol A Polycarbonate. In addition to the T_1(C) compensation, measurement of a reference S_0 allows an interpretation of 2D cross-peak volumes (intensities) by 1D $\Delta S/S_0$ ratios, which are directly related to the numbers of $^{13}C-^{13}C$ pairs involved in exchange. For example, for a mixing time of 200 ms, the 42 ppm quaternary (C_q) carbon of polycarbonate has an average $\Delta S/S_0$ of 3%. This value corresponds to coupling to six carbons (up−up and down−down $^{13}C-^{13}C$ spin pairs do not exchange, and the natural-abundance concentration of ^{13}C is 1%). The 2D CODEX 42 ppm cross peaks (Figure 2) reveal which intrachain carbons are coupled to the C_q carbon. We assign these cross peaks to the two nonprotonated aromatic carbons (Figure 3, top, red) and four protonated aromatic carbons (Figure 3, top, green) that are within two bonds of the C_q carbon within the polycarbonate repeat unit.

The 150 ppm combination of carbons has a cross peak to C_q carbons at a shift difference of 108 ppm, as well as a stronger cross peak to methyl carbons at 120 ppm. The increased intensity of

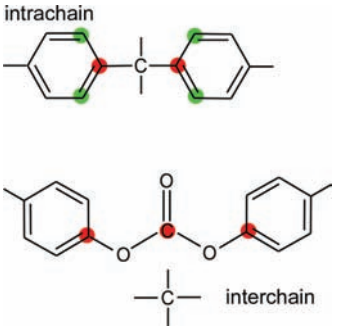

Figure 3. Some intra- and interchain proximities of the quaternary carbon (C_q) of polycarbonate. Because of the steric bulk of an isopropylidene group, only two of the carbons highlighted in red (bottom structure) are on average within 5 Å of the C_q carbon of the nearest-neighbor chain.

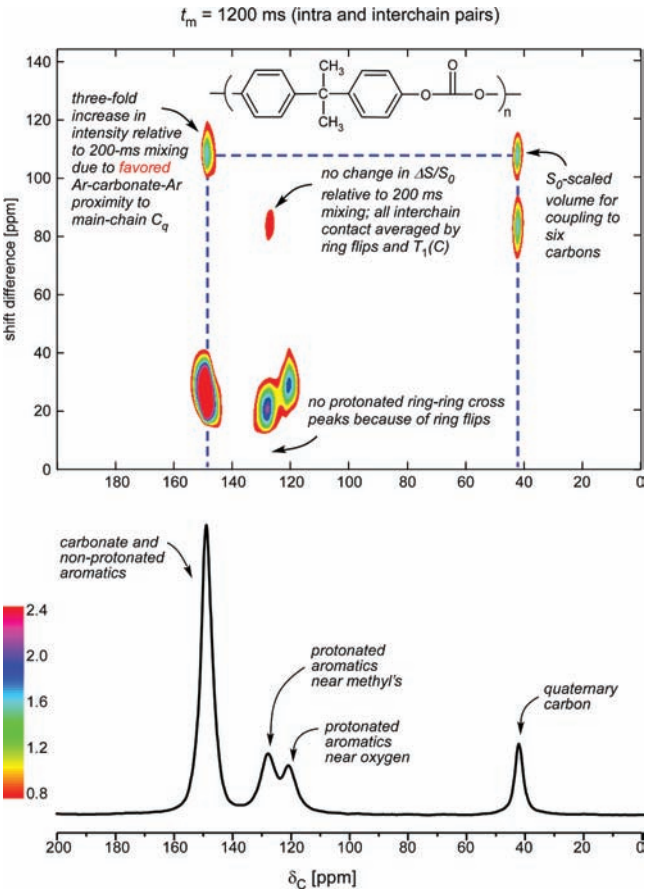

Figure 4. 2D CODEX difference spectrum of bisphenol A polycarbonate using the pulse sequence of Figure S1 with a mixing time of 1200 ms. The 150 ppm−42 ppm cross peaks have both increased in volume by a factor of 3, relative to their values with a 200 ms mixing time (see Figure 2).

the latter results from the proximity of each nonprotonated aromatic carbon to two methyl carbons (Figure 3, top). Methyl carbon cross peaks are not observed directly because of the weak S_0 intensity associated with a short T_1(C).

For a 1200 ms mixing time, the 150 ppm carbon cross peak to methyl carbons has disappeared, while the 42 ppm C_q carbon cross peak to the 150 ppm carbons has increased by a factor of 3

dx.doi.org/10.1021/ja109104f |J. Am. Chem. Soc. 2011, 133, 2626–2631

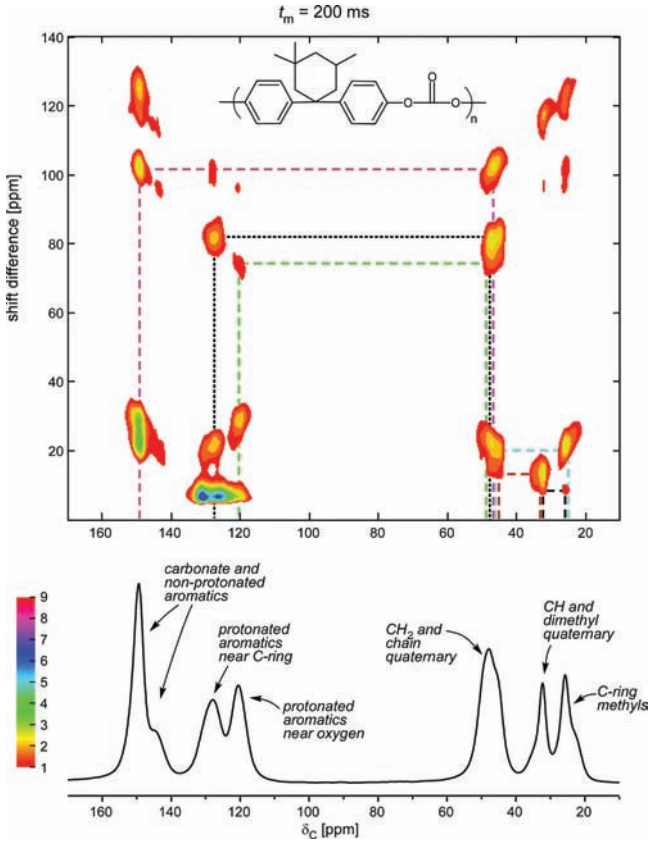

Figure 5. 2D CODEX difference spectrum of trimethylcylcohexyl polycarbonate, using the pulse sequence of Figure S1 with a mixing time of 200 ms. On the basis of cross-peak volumes, the 50 ppm methylene and C_q carbons (see inset for structure) have about equal average intrachain proximities to two methyl carbons (dashed blue square), two 128 ppm protonated aromatic carbons (dotted black square), and two 150 ppm nonprotonated aromatic carbons (dashed red square).

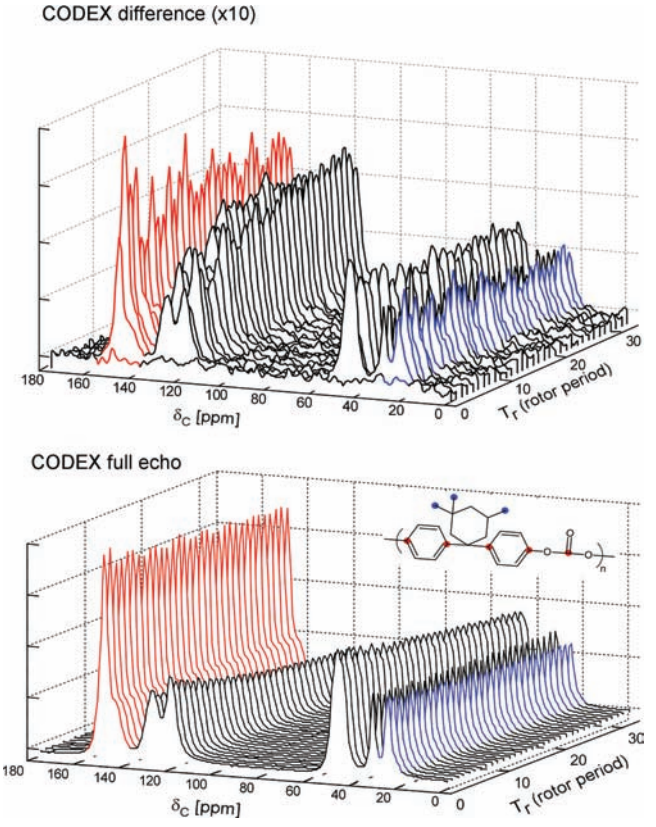

Figure 6. 25 MHz natural-abundance ^{13}C CODEX spectra of trimethylcylcohexyl polycarbonate, using the pulse sequence of Figure S1 with n = 0−32, and a mixing time of 1200 ms. CODEX differences (×10) are shown on top and the full echoes at the bottom. A 1.2 s mixing time results in proton-assisted spin diffusion over distances of about 5 Å. The average $\Delta S/S_0$ of 8% for the methyl peak (blue highlight) means that each methyl is coupled to 16 other ^{13}C's, most of them in nearest-neighbor chains in the glass. Each spectrum was the result of the accumulation of 16K scans. Magic-angle spinning was at 4 kHz.

(Figure 4). That is, there are now six 150 ppm carbons within 5 Å of each C_q carbon. Two of these six carbons are the intrachain nonprotonated carbons already identified in Figure 3 (top, red). Two others are the intrachain nonprotonated carbons that are four bonds distant from C_q. The other two carbons must be interchain. Proximity within 5 Å of Ar−C_q−Ar 150 ppm carbons of one chain, to C_q carbons of an adjacent chain, is not possible because of the steric interference of a pair of isopropylidenes. However, the expectation, based on coarse-grained modeling,[3] is that there is just over one Ar−carbonate−Ar moiety from a nearest-neighbor chain near each C_q carbon. This proximity would result on average in two interchain 150 ppm carbons within 5 Å for each C_q carbon (Figure 3, bottom). Thus, the packing of carbonates of one chain and the isopropylidene of the nearest-neighbor chain in polycarbonate by 2D CODEX is consistent with the nonrandom preferences detected by both REDOR[2] and coarse-grained modeling.[3]

The same preferences in nearest-neighbor packing are also observed directly for the 150 ppm carbons. The 150 ppm cross peak to C_q carbons triples in intensity relative to that for 200 ms mixing, consistent with one set of 150 ppm carbon intrachain couplings (Figure 3, top) and one set of 5 Å interchain couplings (Figure 3, bottom), to each C_q carbon. The simplicity of cross-peak spin counting in 2D CODEX is the direct result of the limitation to static $^1H-^{13}C$ dipolar line broadening[9] of the proton assist to $^{13}C-^{13}C$ spin diffusion. Despite this simplicity, we restrict our analysis to semiquantitative comparisons of nearest-neighbor proximities. More accurate assessments require exact specifications of the locations of all the protons and detailed spin-dynamics simulations, which are beyond the scope of this work.

Trimethylcyclohexyl Polycarbonate. We further illustrate the capabilities of 2D CODEX to determine chain packing semiquantitatively by comparing spectra of trimethylcyclohexyl polycarbonate (TMCPC),[20] a commercial product of Bayer Plastics, with those of bisphenol A polycarbonate.

The most intense cross peak for the cyclohexyl methyl carbons for a short mixing time of 200 ms is to intrachain CH_2 and chain C_q carbons (Figure 5), as expected. A 2D CODEX stack plot for TMCPC with a longer mixing time of 1200 ms is shown in Figure 6. The 25 ppm methyl−carbon peak in Figure 6 has an average 1D $\Delta S/S_0$ ratio of about 8%, which means that each methyl carbon is connected to at least 16 (±2) other carbons. This number is consistent with our expectation of 15−20 carbons within a 1 nm-diameter sphere for a glass density of approximately 1.2 g/cm^3. Its accuracy is determined by the signal-to-noise of ΔS (Figure 6, top) of approximately 10%.

The identity of the 16 carbons coupled to each methyl carbon is revealed by following the vertical blue dotted lines at 25 ppm

dx.doi.org/10.1021/ja109104f |J. Am. Chem. Soc. 2011, 133, 2626–2631

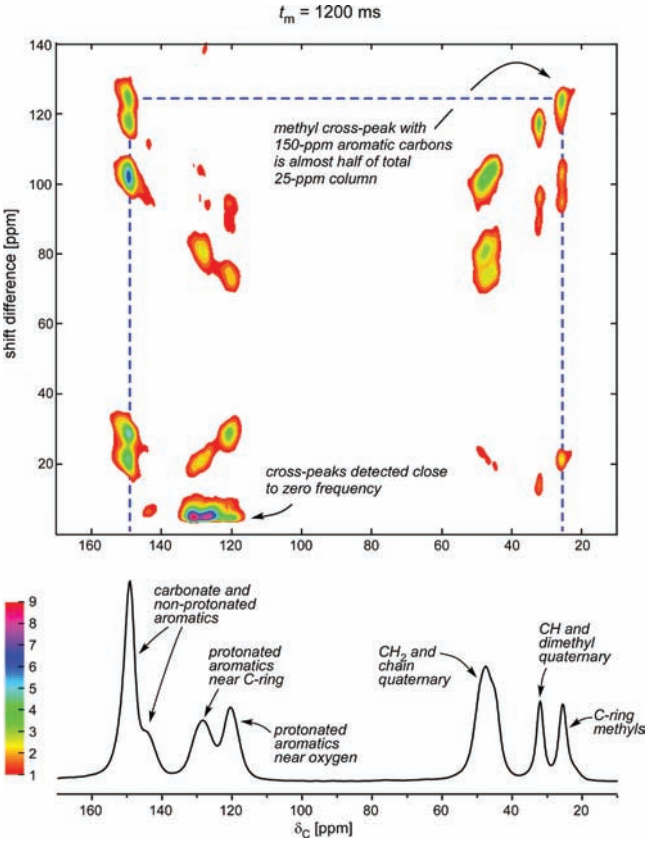

Figure 7. 2D CODEX difference spectrum of trimethylcylcohexyl polycarbonate, using the data of Figure 6, and 32 additional t_1 points at $nt_r/2$. The collection time for all these data was 2 months. The CODEX S and S_0 spectra (see caption to Figure S1) make up the CODEX difference and were collected on alternate scans. This removes the effect of short-term spectrometer instability during long collection periods just as in lengthy REDOR experiments. Some of the couplings between intrachain aliphatic carbons have disappeared because of T_1(C) relaxation. A dashed blue square connects cross peaks at 25 and 148 ppm.

(Figure 7). The most intense cross peak is at 150 ppm. Because only two of the five 150 ppm carbons within a repeat unit are within 5 Å of a methyl carbon, the majority must be in nearest-neighbor chains. In addition, the aromatic-carbon 1D $\Delta S/S_0$ ratios are of the order of 30%, much larger than those of the cyclohexyl ring, with most of the cross-peak volume in the aromatic region (Figure 7). We conclude that the local arrangement of neighboring chains in trimethylcyclohexyl polycarbonate is distinctly nonrandom with a tendency for the cyclohexyl rings to pack near carbonate moieties rich in 150 ppm carbons (see Figure 6, bottom inset, red highlight) rather than to one another, and for the mainchain aromatic rings to stack. Note that the first conclusion is based on a comparison of methyl−carbon to 150 ppm carbon cross peaks for two mixing times. The spin diffusion pathways are therefore similar, and detailed knowledge of the locations of the protons not necessary.

Local Structure and Dynamics. Once a model of the local structure of the polymer glass has been established by variation of t_m to distinguish intra- and interchain nearest neighbors, standard CODEX[4,7] (with recoupling π pulses during t_s), and various rotating-frame and spin−lattice relaxation experiments,[17] can be used to connect molecular dynamics with local chain packing. However, even without these relaxation measurements, the absence of low-frequency aromatic-carbon 2D CODEX cross peaks in polycarbonate (Figure 4), and their presence in the more structurally ordered TMCPC (Figure 7), indicate a greater degree of averaging of dipolar coupling by large-amplitude ring motions like 180° flips in polycarbonate than in TMCPC. Main-chain cooperative motions are necessary to facilitate ring flips,[21] and such main-chain motions are mechanically active.[22] We have argued before that kilohertz-regime slipage motions of polycarbonate main chains relieve the stresses imposed by a sudden impact.[23,24] Thus, the 2D CODEX aromatic-carbon cross-peak intensities of Figures 4 and 7 are consistent with the much higher impact strength[25] (greater ductility) of polycarbonate relative to that of TMCPC.

■ ASSOCIATED CONTENT

Supporting Information. Experimental methods section, which includes a set of figures showing the data processing used to produce a 2D CODEX contour plot for sodium propionate, as well as a table of interatomic distances from the X-ray crystallographic analysis of sodium propionate. This material is available free of charge via the Internet at http://pubs.acs.org.

■ AUTHOR INFORMATION

Corresponding Author
jschaefer@wustl.edu

■ ACKNOWLEDGMENT

We thank Dr. Daniel H. Bolton, Bayer Corp., Plastics Division, for generously providing the polycarbonate samples. The X-ray analysis of sodium propionate was performed by Dr. Nigam P. Rath (Department of Chemistry, University of Missouri at St. Louis).

■ REFERENCES

(1) Gullion, T.; Schaefer, J. *Adv. Magn. Reson.* **1989**, *13*, 57–83.
(2) Stueber, D.; Mehta, A. K.; Chen, Z.; Wooley, K. L.; Schaefer, J. *J. Polym. Sci., Part B: Polym. Phys.* **2006**, *44*, 2760–2775.
(3) Stueber, D.; Yu, T-Y; Hess, B.; Kremer, K.; Schaefer, J. *J. Chem. Phys.* **2010**, *132*, 104901–9.
(4) deAzevedo, E. R.; Hu, W. G.; Bonagamba, T. J.; Schmidt-Rohr, K. *J. Am. Chem. Soc.* **1999**, *121*, 8411–8412.
(5) deAzevedo, E. R.; Franco, R. W. A.; Marletta, A.; Faria, R. M.; Bonagamba, T. J. *J. Chem. Phys.* **2003**, *119*, 2923–2934.
(6) Sharif, S.; Singh, M.; Kim, S. J.; Schaefer, J. *J. Am. Chem. Soc.* **2009**, *131*, 7023–7030.
(7) deAzevedo, E. R.; Hu, W. G.; Bonagamba, T. J.; Schmidt-Rohr, K. *J. Chem. Phys.* **2000**, *112*, 8988–9001.
(8) Meier, B. H. . In *Advances in Magnetic and Optical Resonance*; Warren, W. S., Ed.; Academic Press: New York, 1994; Vol. 18.
(9) Grommek, A.; Meier, B. H.; Ernst, M. *Chem. Phys. Lett.* **2006**, *427*, 404–409.
(10) Ernst, M.; Meier, M. A.; Tuherm, T.; Samoson, A.; Meier, B. H. *J. Am. Chem. Soc.* **2004**, *126*, 4764–4765.
(11) VanderHart, D. L. *J. Magn. Reson.* **1987**, *72*, 13–47.
(12) Manolikas, T.; Herrmann, T.; Meier, B. H. *J. Am. Chem. Soc.* **2008**, *130*, 3959–3966.
(13) Reichert, D.; Bonagamba, T. J.; Schmidt-Rohr, K. *J. Magn. Reson.* **2001**, *151*, 129–135.
(14) Krushelnitsky, A.; Bräuniger, T.; Reichert, D. *J. Magn. Reson.* **2006**, *182*, 339–342.
(15) Hou, S.-S.; Chen, Q.; Schmidt-Rohr, K. *Macromolecules* **2004**, *37*, 1999–2001.

(16) Khitrin, A. K.; Fung, B. M. *J. Magn. Reson.* **2001**, *152*, 185–188.
(17) Schaefer, J.; Sefcik, M. D.; Stejskal, E. O.; McKay, R. A.; Dixon, W. T.; Cais, R. E. *Macromolecules* **1984**, *17*, 1107–1118.
(18) Kaji, H.; Horii, F. *Chem. Phys. Lett.* **2003**, *377*, 322–328.
(19) deAzevedo, E. R.; Bonagamba, T. J.; Schmidt-Rohr, K. *J. Magn. Reson.* **2000**, *142*, 86–96.
(20) Freitag, D.; Fengler, G.; Morbitzer, L. *Angew. Chem., Int. Ed. Engl.* **1991**, *30*, 1598–1610.
(21) Paik, Y.; Poliks, B.; Rusa, C. C.; Tonelli, A. E.; Schaefer, J. *J. Polym. Sci., Part B: Polym. Phys.* **2007**, *45*, 1271–1282.
(22) Chen, L. P.; Yee, A. F.; Goetz, J. M.; Schaefer, J. *Macromolecules* **1998**, *31*, 5371–5382.
(23) Schaefer, J.; Stejskal, E. O.; Perchak, D.; Skolnick, J.; Yaris, R. *Macromolecules* **1985**, *18*, 368–373.
(24) Wu, J.; Xiao, C.; Yee, A. F.; Klug, C. A.; Schaefer, J. *J. Polym. Sci., Part B: Polym. Phys.* **2001**, 1730–1740.
(25) Haggard, K. W.; Paul, D. R. *Polymer* **2004**, *45*, 2313–2320.